TRR
JOURNAL OF THE TRANSPORTATION RESEARCH BOARD

Research Article

Transportation Research Record
2024, Vol. 2678(2) 135–152

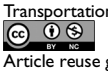

DOI: 10.1177/03611981231172956
journals.sagepub.com/home/trr
Sage

Optimization-Based Intersection Control for Connected Automated Vehicles and Pedestrians

Tanja Niels[1], Klaus Bogenberger[1], Markos Papageorgiou[2], and Ioannis Papamichail[2]

Abstract

Traffic at larger or busier urban intersections is currently coordinated using traffic signals to prevent dangerous traffic situations and to regulate the flow of traffic. In future scenarios with 100% connected automated vehicles, conventional traffic signals could be replaced, and vehicles at intersections could be seamlessly coordinated via vehicle-to-vehicle and vehicle-to-infrastructure communication. In the past two decades, many such control strategies have been presented, commonly referred to as autonomous intersection management (AIM). In recent years, an evolution from simpler first come, first served to more sophisticated optimization-based AIM strategies can be observed. Optimization-based AIM can significantly improve capacity and reduce delays as compared to slot-based strategies and conventional traffic signal control (TSC). In addition, it allows for prioritizing road users. This paper is among the first to consider pedestrians in optimization-based AIM. The proposed approach consists of a signal-free vehicle control in combination with pedestrian signal phases that are fully integrated into the optimization problem. Since the communication range of the controller is limited in real-world applications, a rolling horizon scheme is presented and explained in detail. The presented strategy is implemented and evaluated using a microscopic traffic simulation framework. Results show that vehicle delays can be significantly reduced and vehicle capacity can be increased compared to fully actuated TSC, while pedestrian waiting times are comparable. In addition, focus is put on how vehicle and pedestrian delays can be balanced in the presented setup. Three different control parameters can be adjusted, which need to be tuned based on the considered demand scenario.

Keywords

operations, automated, connected, intelligent transportation system, automated/autonomous/connected vehicles, optimization, pedestrians and bicycles, vehicle-to-infrastructure

Transportation plays a major role in people's everyday lives. Ever-increasing vehicle miles traveled coincide with a growing awareness with respect to the negative impacts of motorized traffic—especially in urban areas. Because of congestion, in more than 200 cities worldwide an average vehicle trip takes 25% more time than in free-flow conditions (*1*). In addition, many cities have to cope with high levels of air pollution, and motorized traffic in cities imposes a risk on pedestrians and bicyclists (*2*). Conflicts predominantly occur at intersection zones, which are the bottlenecks of urban transportation networks. At the same time, new and fast advancing technologies offer several potential solutions that can be combined to mitigate these problems. Automated vehicles (AVs) will be capable of sensing their environments and navigating different traffic conditions with little or no input from the passenger. Connected automated vehicles (CAVs) will additionally be able to communicate with other vehicles and the infrastructure, which makes it possible to coordinate their movements more efficiently. CAVs are thus

[1]Chair of Traffic Engineering and Control, Technical University of Munich, Munich, Germany
[2]School of Production Engineering and Management, Technical University of Crete, Chania, Greece

Corresponding Author:
Tanja Niels, tanja.niels@tum.de

expected to have positive effects on fuel efficiency, congestion reduction, and road safety. This especially applies for intersection zones, where vehicle movements could be orchestrated to improve both safety and efficiency. While traffic at larger or busier urban intersections is currently coordinated using traffic signals to prevent dangerous traffic situations and to regulate the flow of traffic, costly implementation of physical traffic signals might no longer be necessary if all vehicles are connected and automated. With increasing progress in vehicular communication and automation, signal-free intersections have been presented as a possible future vision. In so-called autonomous intersection management (AIM) concepts, vehicles communicate with each other or with infrastructure that is installed at the intersection zone, and reserve a specific time slot or trajectory for crossing the intersection zone safely. The concept promises both safety and efficiency benefits that go beyond traditional traffic signal control (TSC) optimization (*3*). However, this only generally holds true if proper optimization techniques are applied to distribute space–time to different road users. Simple rule-based approaches have been shown to improve vehicle delays in undersaturated conditions but at the same time reduce the capacity at larger intersection zones (*4*, *5*).

Even though signalized intersections predominantly exist in multimodal urban environments, most AIM studies focus on vehicle-only traffic and do not consider pedestrians or bicyclists at the intersection. In previous papers, authors have proposed new integrated intersection control strategies that featured the demand-responsive integration of signal green phases for pedestrians into rule-based AIM (*6*, *7*). This paper extends these studies by (i) applying a more flexible intersection modeling approach, (ii) significantly reducing delays by applying optimization, and (iii) demonstrating how parameter settings can be used to balance vehicle and pedestrian delays. The research is a part of the PhD thesis by Niels (*8*). The paper is structured as follows: the second section presents related literature; the third section explains the applied optimization problem; the fourth section describes the simulation setup; the fifth section discusses the obtained results; and the sixth section concludes the study and gives an outlook on future research topics.

Related Work

The first notable work on AIM was presented by Dresner and Stone (*9*, *10*). They presented a multi-agent approach where vehicle agents communicate with an intersection agent to exclusively reserve discrete areas of the intersection zone. Motivated by the promising results and the continuous development in CAV technology, many studies by scholars from all over the world followed. Several recent surveys (*11–14*) give an overview about the considerable literature in the field. The most important AIM components and typical characteristics are briefly summarized in the following.

Traffic Coordination

Traffic coordination includes the detection and adaptation of conflicting vehicle movements. The traffic coordination at an intersection zone can either be organized with the help of a central controller, or in a cooperative manner, where vehicles communicate with each other and follow a protocol without the need for a central coordination unit. As there is no single point of failure, decentralized AIM is considered to be more robust. On the other hand, it also requires more communication effort to ensure information consistency, and reaching a global objective is more difficult (*11*, *12*). If human drivers, pedestrians, or bicyclists are considered as well, then a central controller is typically assumed, since there is no clear communication protocol with human road users (*6*, *7*, *15–18*).

Intersection Modeling

To identify conflicts between different road user movements, an intersection model is needed. With the exception of very few recent studies (e.g., Li et al. [*19*]), it is assumed that each vehicle follows a predefined path through the intersection that is determined by entrance and exit lanes. To resolve conflicts, the AIM needs to detect vehicle paths that overlap or cross each other and ensure sufficient time gaps between each two vehicles. A common approach when modeling AIM is to first discretize the space of the intersection zone, that is, to divide it into a set of pairwise disjoint cells. Each vehicle passes a subset of these discrete zones in a given order. Now, conflicts can be avoided by limiting the occupancy of each cell to one vehicle at a time (*9*, *10*). A larger number of cells increases the accuracy of the considered reservations and can improve the efficiency of the control, but also increases the complexity of the calculation (*20*, *21*). Zhu and Ukkusuri (*22*) propose to instead generate a matrix that indicates whether two paths intersect and includes the exact distances between conflict points. Then, two vehicles with conflicting movements are allowed in the intersection zone at the same time if sufficient spacing between these two vehicles at their conflict point can be guaranteed (*17*, *22*, *23*).

Scheduling Policy

The scheduling policy describes how the order and arrival times of vehicles entering the intersection zone are determined. One of the most widely used concepts is the

Table 1. Literature on the Integration of Pedestrians into Autonomous Intersection Management (AIM)

Paper	Year	Traffic coordination	Integration of pedestrians	Microscopic simulation	Evaluation of pedestrian delay	Approach
Dresner and Stone (*15*)	2008	Rule-based	Pre-timed	No	No	Combination of FCFS-based vehicle control with pre-timed TSC
Niels et al. (*6*, *7*)	2019, 2020	Rule-based	Demand-resp.	Yes	Yes	Integration of pedestrians into rule-based AIM
Chen et al. (*16*)	2020	Opt.-based	Demand-resp.	No	Limited	Integration of pedestrians into AIM with max-pressure control
Wang et al. (*17*)	2021	Opt.-based	Demand-resp.	Yes	No	Integration of pedestrians and spillback into optimization-based AIM
Wu et al. (*18*)	2022	Opt.-based	Demand-resp.	No	Yes	Pedestrians use autonomous shuttles to cross the intersection

Note: Opt. = optimization; resp. = responsive; FCFS = first come, first served; TSC = traffic signal control.

first come, first served (FCFS) strategy, also known as first in, first out. As the name suggests, it processes requests of approaching vehicles in the order of their receipt. FCFS is easy to implement and can provide an immediate response for the vehicle that has requested passage. However, FCFS schemes can be inefficient, as they do not take advantage of the knowledge the system has about arriving vehicles. Levin et al. (*4*) found several situations in which traditional traffic signals outperformed the FCFS approach. In addition, the strict paradigm of FCFS does not allow for prioritization of vehicles. Several rule-based extensions have been proposed to overcome these issues, for example, by applying auctions (*24*, *25*) or considering platoons as one entity (*26*). To further improve the efficiency and flexibility of AIM, optimization-based scheduling policies have been presented. They are usually formulated as mixed-integer linear programs (MILPs) with the objective of minimizing the sum over all vehicle delays (*23*, *27*, *28*). Yu et al. (*5*) show that optimization-based AIM significantly outperforms FCFS schemes.

Integration of Pedestrians into AIM

While the AIM approaches presented in the literature so far could lead to a more efficient use of intersection space in the future, the continuous vehicle movement infringes pedestrian and bicyclist possibilities to cross the intersection. This is a major difference to traditional TSC, which grants the right-of-way in an alternating fashion. Even though the focus of signal timing often lies on vehicle traffic, the phase-based principle of traffic signals allows pedestrians to cross the intersection together with parallel vehicle movements. In contrast, AIM approaches are vehicle-based, that is, each vehicle is given the right-of-way individually on request. If no space–time is requested by or on behalf of pedestrians, there will be no green phase that they can be appended to. Therefore, they need to be considered explicitly in the reservation process. Nevertheless, pedestrians have been considered in very few studies on AIM so far.

An overview on AIM studies featuring the integration of pedestrians is shown in Table 1. Pedestrian integration is especially challenging because pedestrians are currently not connected to other road users or the infrastructure, and therefore their speeds and desired destinations are not easily predictable. These issues have been discussed in detail by Niels et al. (*6*, *7*) and new rule-based control strategies have been proposed. To provide a safe, practical, and user-friendly system, the considered intersections were equipped with infrastructure to detect pedestrians and show them when they are given the right-of-way. The presented results were very promising, but the disadvantages of FCFS-based control were apparent when considering large vehicle and pedestrian demand. Both Chen et al. (*16*) and Wang et al. (*17*) describe the integration of pedestrian right-of-way into optimization-based AIM. However, the studies do not include pedestrians in the simulation or provide limited results that, because of restrictive assumptions, do not allow for a comprehensive comparison with state-of-the-art TSC. In addition, the presented MILP formulations can be adapted with weighting factors (*16*,*23*), which to the best of our knowledge has not been explored as a means to balance road user delays yet.

Contributions of this Study

This paper provides a detailed evaluation on how vehicle and pedestrian delays can be balanced in optimization-

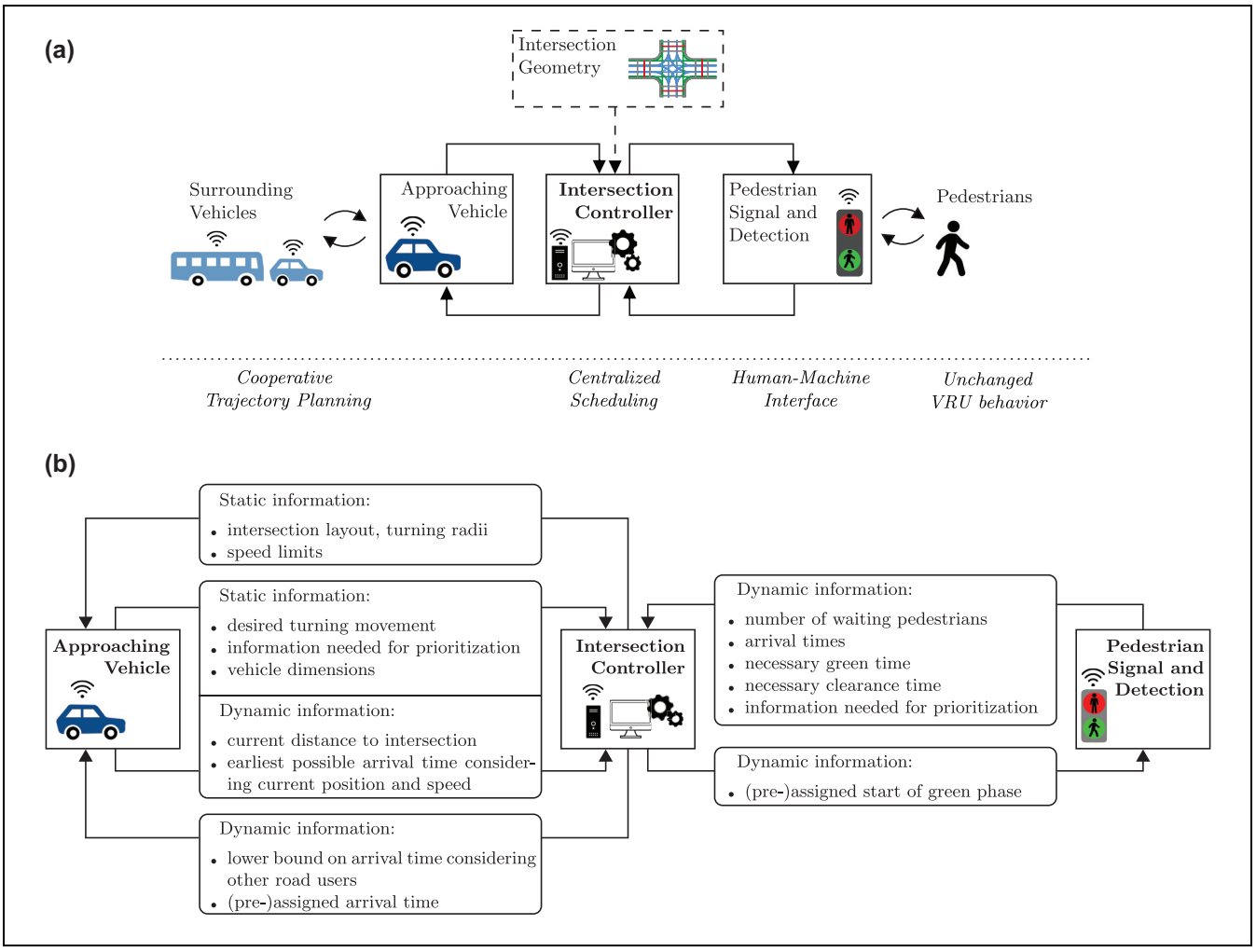

Figure 1. Overall control architecture and communication setup: (*a*) control architecture of the proposed autonomous intersection management scheme and (*b*) communication among the intersection controller, vehicles, and pedestrian infrastructure.

based AIM. To account for practical constraints, such as limited communication distances and pedestrians not being equipped with connected devices, a rolling horizon approach is presented and explained in detail. The approach is implemented and evaluated using a microsimulation platform, and a direct comparison to fully actuated TSC is provided.

Methodology

This section presents the intersection control applied in this paper. It follows the same structure as the previous one with a focus on the consideration of pedestrians in each of the components.

Traffic Coordination

As displayed in Figure 1*a*, the control scheme presented in this paper consists of a central controller that schedules all arriving road users while trajectories are planned by vehicles. Pedestrians are assumed to behave "naturally," that is, no trajectories are planned for them, but they react to the pedestrian signals that can look and work like today and serve as a human–machine interface.

Approaching vehicles communicate directly with the intersection control; the exchanged information is displayed in Figure 1*b*. The intersection controller first provides the approaching vehicles with the static information needed to plan their trajectory, such as the exact geographic position of the entrance to the intersection zone and relevant speed limits. With this information, vehicles can derive their earliest possible arrival time at the entrance to the intersection depending on the current position and speed. This information is needed to assign a feasible time slot for the vehicle and to calculate the vehicle's delay. To simplify the control, it is assumed that all vehicles cross the intersection at the same constant speed. On the approach to the intersection, each vehicle

keeps the controller updated about whether the earliest possible arrival time at the intersection has changed. It has to be noted that this arrival time is an ego perspective of the vehicle without considering other road users. On the other hand, the intersection control entity returns to the vehicle a lower bound on its scheduled arrival time that considers other previously scheduled road users. If the vehicle arrival time has been fixed, the assigned arrival time is sent to the vehicle. The vehicle adjusts its speed on the approach to the intersection zone individually while making sure that it arrives at the intersection zone with the predefined speed.

Pedestrians are assigned to signal phases and assumed to cross the intersection together when given the right-of-way. This setup aims at not forcing pedestrians to have to adapt their current behavior in the futuristic setup. In particular, they are not required to wear connected devices. To fully integrate pedestrian signal activation into the optimization problem, pedestrians are detected when they arrive at the crosswalk. The intersection controller continuously receives information about waiting pedestrians, necessary green times, clearance times, and information that is needed for prioritization. The communication between the intersection controller and pedestrian infrastructure is also displayed in Figure 1*b*.

Intersection Modeling

This study applies a conflict point-based approach that facilitates the integration of heterogeneous vehicle dimensions and the transferability to other intersection layouts. As described in the second section, all road users are assumed to roughly travel through the intersection along predefined paths. With these paths, conflict points among merging, diverging, and crossing movements can be determined. Figure 2*a* shows the intersection considered in this paper. It presents all allowed paths for vehicles (blue) and pedestrians (red), and displays conflict points for selected movements. For reasons of simplicity, the intersection does not feature the diagonal crossing of pedestrians. Bicycle movements are shown in the figure (green), but their consideration will be left for future analyses.

The conflicts between different road users do not only have to be resolved at the one-dimensional points shown in Figure 2*a*, but each two conflicting movements span a conflict area. Examples of vehicle–vehicle conflict areas are shown in Figure 2*b*. It is easy to see that the size of the conflict region depends on how the vehicle paths overlap. Therefore, they are spanned dynamically with information on vehicles' origins and destinations. Figure 2*c* shows a vehicle–pedestrian conflict region. From the vehicle perspective, the conflict region includes the entire width of the pedestrian crosswalk; from the pedestrian

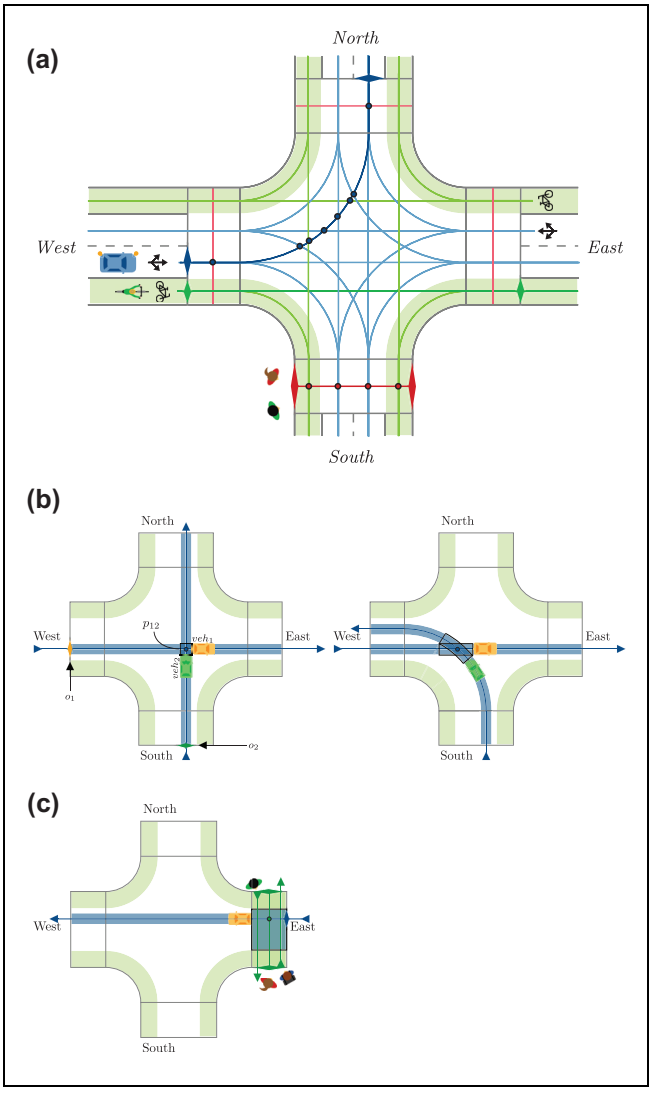

Figure 2. Considered intersection layout and example conflict points and regions: (*a*) considered intersection zone with paths and conflict points of different road users, (*b*) conflict regions of different vehicle–vehicle conflicts, and (*c*) example conflict region of vehicle–pedestrian conflict (color online only).

perspective, it includes the entire width of the vehicle road. To resolve conflicts, only one vehicle or a group of pedestrians is allowed within the spanned conflict region at a time. Vehicle arrival times and start times of pedestrian green phases are determined such that the second road user only enters the conflict region after the first road user has left and a sufficient time gap $\delta^{\min}$ has passed. The extensions of the two-dimensional conflict regions are taken into account with larger time gaps $\Delta^{\min}$ that include the time spent within the conflict region. Let o_i and o_j be the points where vehicles veh_i and veh_j enter the intersection (diamond shapes in Figure 2*b*), and let p_{ij} be their common conflict point. Furthermore, let t_i and t_j be the times that they enter the intersection zone

and v_{veh} be their speed. Then veh_i arrives at the conflict point at time $t_i + \frac{dist_{o_i,p_{ij}}}{v_{veh}}$, where $dist_{o_i,p_{ij}}$ is the distance between o_i and p_{ij} following the vehicle path. The time veh_j arrives at the conflict point can be calculated analogously. Now, the following needs to be ensured:

$$\begin{aligned} & t_i + \frac{dist_{o_i,p_{ij}}}{v_{veh}} \geqslant t_j + \frac{dist_{o_j,p_{ij}}}{v_{veh}} + \Delta_{ji}^{\min} \\ & \text{if } t_i + \frac{dist_{o_i,p_{ij}}}{v_{veh}} \geqslant t_j + \frac{dist_{o_j,p_{ij}}}{v_{veh}} \end{aligned} \tag{1}$$

or:

$$\begin{aligned} & t_j + \frac{dist_{o_j,p_{ij}}}{v_{veh}} \geqslant t_i + \frac{dist_{o_i,p_{ij}}}{v_{veh}} + \Delta_{ij}^{\min} \\ & \text{if } t_j + \frac{dist_{o_j,p_{ij}}}{v_{veh}} > t_i + \frac{dist_{o_i,p_{ij}}}{v_{veh}} \end{aligned} \tag{2}$$

depending on which vehicle passes the conflict point first.

A similar approach applies for conflicts with vehicles and pedestrians. The difference is that pedestrian speeds are not known beforehand, and pedestrians crossing the same leg are supposed to cross the intersection zone roughly at the same time, that is, when their respective signal head turns green. Based on this assumption, it does not make sense to consider each individual pedestrian separately, but space is instead reserved for signal phases. Let sig_m be a pedestrian signal phase that starts at time t_m and let p_{im} be the conflict point of the corresponding pedestrian movement and vehicle veh_i. To fulfill the objective of developing a control scheme that is easily understandable and safe for everyone, vehicles should have left the pedestrian crosswalk when the signal turns green. Therefore, no "start up time" is considered for pedestrians, and $dist_{o_m,p_{im}}$ is set to zero. If the green phase is supposed to start after the vehicle has left, the following needs to hold:

$$\begin{aligned} & t_m \geqslant t_i + \frac{dist_{o_i,p_{im}}}{v_{veh}} + \Delta_{im}^{\min} \\ & \text{if } t_m \geqslant t_i + \frac{dist_{o_i,p_{im}}}{v_{veh}} \end{aligned} \tag{3}$$

Otherwise, the constraint is formulated as follows:

$$\begin{aligned} & t_i + \frac{dist_{o_i,p_{im}}}{v_{veh}} \geqslant t_m + \Delta_{mi}^{\min} \\ & \text{if } t_i + \frac{dist_{o_i,p_{im}}}{v_{veh}} > t_m \end{aligned} \tag{4}$$

where Δ_{mi} incorporates the green phase duration and the time it takes for an assumed slowly walking pedestrian to cross the road (clearance time). As described in the following, the scheduling policy will decide which road user passes the conflict point first.

Scheduling Policy

The scheduling policy is the center of the intersection control. It combines all relevant information and applies optimization techniques to achieve the objective of providing a safe and efficient schedule for road users to cross the intersection. As described above, the decision variables will be the arrival time of vehicle *veh* at the entrance to the intersection zone (denoted by t_{veh}) and the start of the green phase for signal phase *sig* (denoted by t_{sig}). Before formally defining the optimization problem, it needs to be noted that the controller does not have perfect knowledge from the start, but can consider vehicles as they sign up and pedestrians as they are detected by the infrastructure (see Figure 1). Therefore, a rolling horizon approach is implemented, and the optimization problem is modeled repeatedly with the information that is currently available. In the following, the approach will be explained for vehicle-only scenarios before the integration of pedestrians is described.

Rolling Horizon Approach for Vehicle-Only Scenarios. Considering a vehicle-only scenario, the available information corresponds to the information of all vehicles that are currently communicating with the intersection controller. The level of information thus depends on the communication range $dist^C$ of the controller and on the length of the approach to the intersection. This is schematically displayed in Figure 3*a*, where the controller can consider the arrival times of the blue vehicles in the optimization problem. At the same time, some of the vehicles (colored orange in Figure 3*a*) have already started crossing the intersection zone or are about to do that, and their arrival times should not be changed any more. This is reflected by defining an assignment distance $dist^A$, after which the arrival times of vehicles are fixed. It is clear that vehicles that have not yet left the intersection still need to be considered in the optimization problem as constraints for safety reasons (i.e., they still block conflict regions). Vehicles that are not considered in the current scheduling process at all are colored gray in Figure 3*a*.

Figure 3*b* shows how these distance-wise considerations relate to the temporal dimension that is usually considered in rolling horizon approaches, and common terms such as "roll period" and "projection horizon" are displayed. The figure schematically shows trajectories of vehicles on the approach to and within the intersection zone. It is assumed that the optimization problem is run in fixed intervals of ϕ s, which corresponds to a fixed roll period. At the time the problem is solved (denoted as t^1, t^2, etc., in Figure 3*b*), the controller takes a snapshot of the situation. The information of the blue and orange vehicles is then considered in the optimization as described above. The number of vehicles considered as

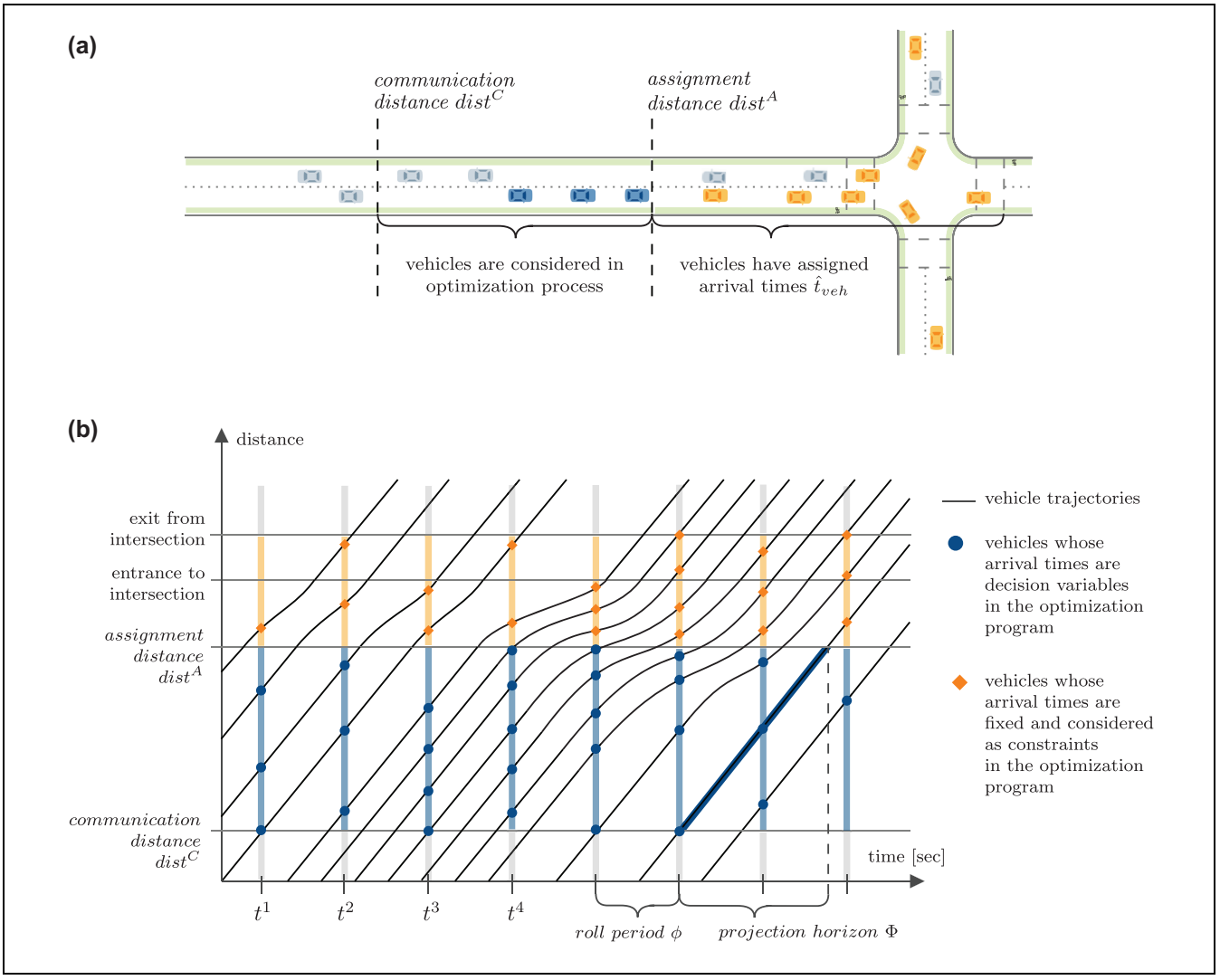

Figure 3. Representation of the relationship between spatial distance and time horizon: (*a*) schematic representation of communication distance and assignment distance and (*b*) example trajectories and schematic representation of the roll period ϕ and projection horizon Φ (color online only).

decision variables thus depends on the length of the stretch between $dist^C$ and $dist^A$, on the number of incoming lanes, and on the vehicle densities in these lanes. In the figure, $dist^C$ and $dist^A$ remain fixed, but the densities change: at time t^1, only three blue vehicles are considered in the optimization problem; at time t^4, there are five blue vehicles in the considered area. Formally speaking, let $t^k = k \times \phi$ for $k \geqslant 0$ denoting the times at which the optimization problem is modeled and solved. It is assumed that, at time t^k, the controller has (i) a list of all vehicles with a fixed time slot $\hat{t}_{veh}$ that have not yet left the intersection (orange vehicles in Figure 3*a*), denoted by $\hat{V}^k$, and (ii) a list of all vehicles within the communication distance but without a fixed time slot (blue vehicles in Figure 3*b*), denoted by V^k. Both lists contain all information that is necessary to safely schedule the newly arriving vehicles. Impacts of a changing communication distance $dist^C$ will briefly be discussed in the *Results and Discussion* section.

Integration of Pedestrians. In contrast to vehicles, pedestrians are detected when they are already at the intersection. A flowchart of the overall procedure is shown in Figure 4*a*: if pedestrians arrive during a green phase, they can immediately start crossing. Otherwise, they are assigned to an already requested signal phase *sig* or, if their signal is currently red and there are no other pedestrians waiting, a new green phase *sig* is requested and the pedestrian is assigned to this new green phase.

Figure 4*b* shows the three situations described above in the rolling horizon setup. It schematically displays the

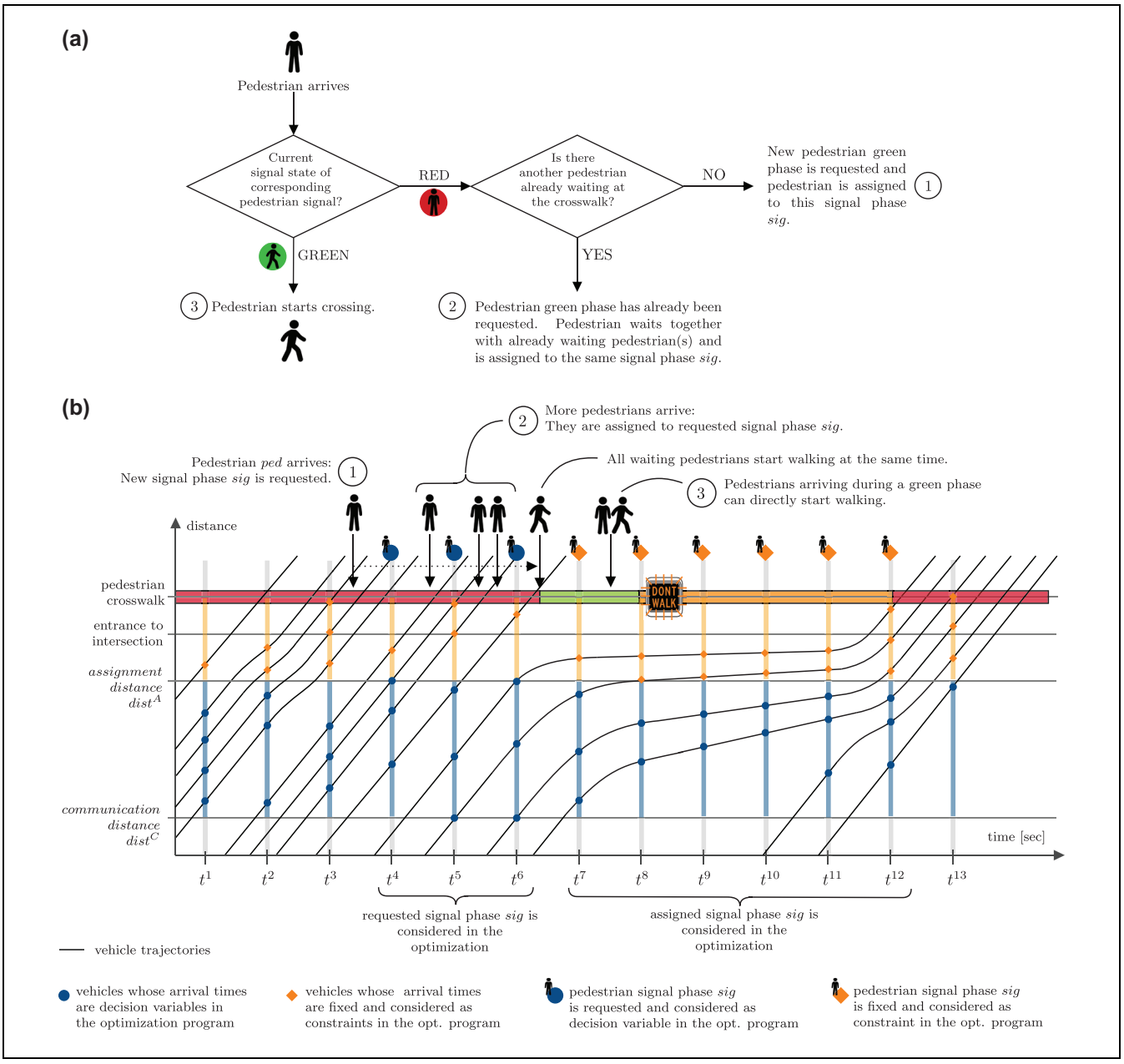

Figure 4. Flowchart and schematic representation of on-demand integration of pedestrian signal phases: (*a*) flowchart of on-demand integration of pedestrians and (*b*) example trajectories and schematic representation of the consideration of a requested pedestrian signal phase (color online only).

trajectories of vehicles on the approach to and within the intersection zone (similar to Figure 3*b*) and the on-demand integration of a pedestrian signal phase. As explained above, the optimization problem is run in fixed intervals of ϕ s, that is, at times $t^k = k \times \phi$ that are displayed on the x -axis. Again, at time t^k, the controller takes a snapshot of the current situation, which is marked vertically. In addition to approaching vehicles, it now also considers requested signal phases in the optimization problem. It can easily be seen that, in contrast to the vehicle case, no look-ahead time is used for pedestrians. In particular, in the situation shown in the figure, no pedestrian green phase is considered when the optimization problem is run at times t^1, t^2, and t^3. The first pedestrian *ped* to request a pedestrian green phase *sig* arrives shortly after t^3, denoted as Situation ① in the figure. Pedestrian *ped* is assigned to the newly requested signal phase *sig*, that is, $ped \in P_{sig}$. The start time of *sig* is first considered as a decision variable in the optimization problem at time t^4 (depicted by the larger blue dot).

Depending on the objective function and necessary constraints that will be explained in the following sections, green phase *sig* is scheduled after at least one round of optimization. Note that those vehicles that already have an assigned arrival time or are currently crossing the intersection (depicted as orange diamonds) cannot be rescheduled. Therefore, depending on the vehicle demand, if the signal is red on the arrival of *ped*, a waiting time that allows assigned vehicles to finish crossing will occur. In the situation shown in the figure, the green phase is scheduled shortly after t^6. In the meantime, more pedestrians arrive and are assigned to the same signal phase *sig*, denoted as Situation ② in the figure. Finally, when the signal green phase starts, all waiting pedestrians are allowed to start walking at the same time. If pedestrians arrive during the green phase, they can start walking without any waiting time (compare Situation ③). Current or recently ended green phases still need to be considered in the optimization problem with necessary constraints to ensure safe crossing for all assigned pedestrians. This is depicted by the large orange diamond shapes in the figure. Overall, the integrated optimization problem at time t^k is set up similarly to the optimization problem for vehicle-only scenarios. In addition to the lists V^k and $\hat{V}^k$ explained above, the controller now has two new lists with requested (S^k) and assigned or current signal phases ($\hat{S}^k$).

Objective Function. The control delay per vehicle or pedestrian, respectively, is the decisive parameter to evaluate the level of service (LOS) at signalized intersection zones according to both the American Highway Capacity Manual (HCM) (*29*) and its German counterpart (*30*). It is also the most widely used performance indicator when evaluating AIM strategies (*14*). Similar to other studies (*17*, *27*), the presented scheduling policy therefore aims at minimizing the sum over all delays. To balance delays and prioritize user groups, delays are additionally weighted in the objective function. For each vehicle *veh*, the control delay is calculated as the difference between the earliest possible arrival time of *veh* at the intersection (denoted by $t_{veh}^{\min}$) and the time it actually enters the intersection area (denoted by t_{veh}). The weighted delay of vehicle *veh* can thus be expressed as follows:

$$\gamma_{veh} \cdot delay_{veh} = \gamma_{veh} \cdot \left(t_{veh} - t_{veh}^{\min}\right) \tag{5}$$

where γ_{veh} denotes the weighting factor of *veh*. Delays of pedestrians are approximated in a similar way. If the pedestrian signal is already green on the arrival of *ped*, then $delay_{ped}$ is zero. Otherwise, pedestrian *ped* is assigned to a requested signal phase as described above. Let $t_{ped}^{\min}$ be the time that pedestrian *ped* arrives at the pedestrian crosswalk and t_{sig} be the time that the signal turns green and *ped* is allowed to start crossing the street. Then, $delay_{ped}$ is defined as $t_{sig} - t_{ped}^{\min}$. The delay and weighting factor of *sig* represents the delays and weighting factors of all pedestrians assigned to *sig*, that is:

$$\gamma_{sig} \cdot delay_{sig} = \sum_{ped \in P_{sig}} \gamma_{ped} \cdot \left(t_{sig} - t_{ped}^{\min}\right) \tag{6}$$

Overall, the objective function at time t^k can be defined as follows:

$$\min\left(\sum_{i \in V^k} \gamma_i \cdot delay_i + \sum_{m \in S^k} \gamma_m \cdot delay_m\right) \tag{7}$$

Constraints. When the optimization problem is set up at time t^k, the constraints need to ensure physical limitations of vehicles approaching the intersection and resolve conflicts with already scheduled and requested vehicle arrival times and signal phases, as explained in the previous section. The logical conditions in Equations 1–4 cannot directly be included into the optimization problem. In general, an optimization model requires that all constraints need to be fulfilled at the same time. Therefore, binary variables $I_{ij} \in \{0, 1\}$ are introduced, where I_{ij} indicates whether road user i is supposed to arrive at the conflict point p_{ij} before road user j. In addition, the multiplication with a large scalar M makes irrelevant constraints redundant. A detailed description of the so-called Big-M method can be found in Williams (*31*). Finally, delays of individual road users can be bounded by suitable upper bounds Θ_{veh} and Θ_{ped}. All in all, the optimization problem can be defined as follows, where the "translation" of the mathematical constraints will be described below.

Problem 1. Intersection control optimization for scenarios with vehicles and pedestrians at time t^k:

$$\min\left(\sum_{i \in V^k} \gamma_i \cdot delay_i + \sum_{m \in S^k} \gamma_m \cdot delay_m\right)$$

subject to

$$\gamma_i \cdot delay_i = \gamma_i \cdot (t_i - t_i^{\min}) \qquad \forall i \in V^k$$

$$\gamma_m \cdot delay_m = \sum_{ped \in P_m} \gamma_{ped} \cdot \left(t_m - t_{ped}^{\min}\right) \qquad \forall m \in S^k$$

$$t_i \geq t_i^{LB}(t^k) \qquad \forall i \in V^k \tag{8}$$

$$t_m \geq t^k \qquad \forall m \in S^k \tag{9}$$

$$t_i \leq t_i^{\min} + \Theta_i \qquad \forall i \in V^k \tag{10}$$

$$t_m \leq t_{sig}^{\min} + \Theta_m \qquad \forall m \in S^k \quad (11)$$

$$t_i \geq t_j + \Delta_{ji}^{\min} \qquad \forall i,j \in V^k \mid o_i = o_j \;\&\; t_i^{\min} > t_j^{\min} \quad (12)$$

$$t_i \geq \hat{t}_l + \Delta_{li}^{\min} \qquad \forall i \in V^k, l \in \hat{V}^k \mid o_i = o_l \quad (13)$$

$$t_i + \frac{dist_{o_i,p_{ij}}}{v_{veh}} + \Delta_{ij}^{\min} \leq t_j + \frac{dist_{o_j,p_{ij}}}{v_{veh}} + (1 - I_{ij}) \times M \qquad \forall i,j \in V^k \quad (14)$$

$$t_i + \frac{dist_{o_i,p_{ij}}}{v_{veh}} + I_{ij} \times M \geq t_j + \frac{dist_{o_j,p_{ij}}}{v_{veh}} + \Delta_{ji}^{\min} \qquad \forall i,j \in V^k \quad (15)$$

$$t_i + \frac{dist_{o_i,p_{im}}}{v_{veh}} + \Delta_{im}^{\min} \leq t_m + \frac{dist_{o_m,p_{im}}}{v_{veh}} + (1 - I_{im}) \times M \qquad \forall i \in V^k, m \in S^k \quad (16)$$

$$t_i + \frac{dist_{o_i,p_{im}}}{v_{veh}} + I_{im} \times M \geq t_m + \frac{dist_{o_m,p_{im}}}{v_{veh}} + \Delta_{mi}^{\min} \qquad \forall i \in V^k, m \in S^k \quad (17)$$

$$t_i + \frac{dist_{o_i,p_{il}}}{v_{veh}} + \Delta_{il}^{\min} \leq \hat{t}_l + \frac{dist_{o_l,p_{il}}}{v_{veh}} + (1 - I_{il}) \times M \qquad \forall i \in V^k, l \in \hat{V}^k \quad (18)$$

$$t_i + \frac{dist_{o_i,p_{il}}}{v_{veh}} + I_{il} \times M \geq \hat{t}_l + \frac{dist_{o_l,p_{il}}}{v_{veh}} + \Delta_{li}^{\min} \qquad \forall i \in V^k, l \in \hat{V}^k \quad (19)$$

$$t_i + \frac{dist_{o_i,p_{in}}}{v_{veh}} + \Delta_{in}^{\min} \leq \hat{t}_n + (1 - I_{in}) \times M \qquad \forall i \in V^k, n \in \hat{S}^k \quad (20)$$

$$t_i + \frac{dist_{o_i,p_{in}}}{v_{veh}} + I_{in} \times M \geq \hat{t}_n + \Delta_{ni}^{\min} \qquad \forall i \in V^k, n \in \hat{S}^k \quad (21)$$

$$t_m + \Delta_{ml}^{\min} \leq \hat{t}_l + \frac{dist_{o_l,p_{lm}}}{v_{veh}} + (1 - I_{ml}) \times M \qquad \forall m \in S^k, l \in \hat{V}^k \quad (22)$$

$$t_m + I_{ml} \times M \geq \hat{t}_l + \frac{dist_{o_l,p_{lm}}}{v_{veh}} + \Delta_{lm}^{\min} \qquad \forall m \in S^k, l \in \hat{V}^k \quad (23)$$

$$I_{ij} \in \{0,1\} \qquad \forall i,j \in V^k \quad (24)$$

$$I_{im} \in \{0,1\} \qquad \forall i \in V^k, m \in S^k \quad (25)$$

$$I_{il} \in \{0,1\} \qquad \forall i \in V^k, l \in \hat{V}^k \quad (26)$$

$$I_{in} \in \{0,1\} \qquad \forall i \in V^k, n \in \hat{S}^k \quad (27)$$

$$I_{ml} \in \{0,1\} \qquad \forall m \in S^k, l \in \hat{V}^k \quad (28)$$

Equations 8 ensure that each arriving vehicle i is not scheduled earlier than the time it can physically be at the intersection considering its current position and speed, denoted by $t_i^{LB}(t^k)$, and Equations 9 ensure that the requested signal phases cannot start earlier than the current time t^k. Vehicle delays and pedestrian waiting times are bounded via Equations 10 and 11. Equations 12 and 13 ensure that vehicles on the same approach do not overtake. Conflicts between arriving vehicles are resolved by Equations 14 and 15, while conflicts between arriving vehicles and requested signal phases are resolved by Equations 16 and 17. Equations 18 and 19 resolve conflicts between arriving and scheduled vehicles, Equations 20 and 21 resolve conflicts between arriving vehicles and scheduled signal phases, and Equations 22 and 23 resolve conflicts between requested signal phases and scheduled vehicles. Equations 24–28 ensure that auxiliary matrices used for the Big-M method are binary.

For the optimization-based intersection control with vehicles only, Levin and Rey (*23*) show that the problem is feasible if delays are not bounded, that is, excluding Equations 10. Their proof can easily be extended to the scenario with vehicles and pedestrians. However, it is not possible to guarantee that a feasible solution with restrictive upper bounds on delays and pedestrian waiting times is found. In the scheme implemented in this paper, the upper bounds on vehicle delays Θ_{veh} are chosen in such a way that Equations 10 are redundant. In addition, if the conflicting movements do not allow activating a certain signal phase *sig* within the next Θ_{sig} s, then Equations 11, which are not safety-critical, are relaxed. In the scenarios presented in the *Results and Discussion* section, this was not the case. If the problem has multiple solutions, a random one is chosen.

Simulation Setup

The presented strategy is implemented and tested using a microsimulation framework: road user arrivals and movements are simulated using Aimsun Next, which is connected to Python via the application programming interface (API). The Python program contains the rules for controlling the intersection and adjusting vehicle trajectories. The Gurobi optimization solver is used to set up and solve the optimization problem. Simulations are run for 60 min, including 10 min of warm-up time, and with five random seeds per scenario. All parameters described in the following are listed in Table 2. Minimum time gaps are set based on literature assumptions for the safe car-following behavior of CAVs (*32*) and all vehicle parameters are comparable to previous studies (*6*, *7*).

The intersection displayed in Figure 2*a* is simulated in this paper. Given the small size of the intersection and

Table 2. Parameter Values for the Test Scenarios

Input parameters	Values
Vehicle parameters	
Vehicle dimensions ($len_{veh} \times wid_{veh}$)	4.0 m×2.0 m
Maximum allowed speed v^{max}	8.3 m/s (30 km/h)
Vehicle speeds for crossing the intersection $\hat{v}_{veh}$	8.3 m/s (30 km/h)
Min. and max. acceleration $acc^{min}\|acc^{max}$	-4.0 m/s^2|3.0 m/s^2
Min. gaps for car-following and crossing movements $\delta^{min}_{follow}\|\delta^{min}_{cross}$	0.7s|1.0 s
Pedestrian parameters	
Min. and max. pedestrian speeds $v^{min}_{ped}\|v^{max}_{ped}$	0.8 m/s|1.5 m/s
AIM control parameters	
Assignment distance $dist^A$	50.0 m
Communication distance $dist^C$ in vehicle-only scenarios	100.0 m
Communication distance $dist^C$ in scenarios with vehicles and pedestrians	150.0 m
Roll period ϕ	3.0 s
Maximum pedestrian waiting time Θ_{ped}	42.0 s
Green phase duration t^{green}_{sig}	5.4 s
Weighting factors $\gamma_{veh}\|\gamma_{ped}$	1.0
TSC control parameters	
Minimum and maximum green phase durations	22.0 s|52.0 s
Yellow phase | All-red phase	3.0 s|5.0 s
Other parameters	
Simulation time step τ | Simulation duration | Warm-up phase	0.6 s|60.0 min|10.0 min
Number of random seeds	5

Note: AIM = autonomous intersection management; Max. = maximum; Min. = minimum; TSC = traffic signal control.

the importance of pedestrian movement, a speed limit of 30 km/h is assumed. To simplify the result discussion, it is assumed that all passenger vehicles have the same dimensions, kinematic limitations, and desired speeds. For the calculation of clearance times in the AIM, pedestrian walking speed is assumed to be 0.8 m/s, which is just below the 10th percentile of low-density walking speeds obtained from field measurements as reported by Hoogendoorn and Daamen (*33*). This is relatively slow as compared to the assumption of 1.2 m/s in the German TSC guideline, RiLSA (*34*). However, it needs to be noted that vehicles will arrive at the intersection at a higher speed in the AIM scenario. Therefore, pedestrian crosswalks need to be monitored by sensors. If pedestrians are detected on the street during a red phase, for example, because they are walking more slowly than expected or because of jaywalking, approaching vehicles need to slow down and request a new time slot for crossing the intersection.

Demand Scenarios

The vehicle demand scenarios are shown in Figure 5*a*. The scenarios are symmetric, that is, demand on all approaches is identical. Some 75% of the vehicles on each approach are through movement, 10% turn left, and 15% turn right. The total number of vehicles that cross the intersection per hour is denoted by the variable x. Pedestrian demand is assumed to be 200 pedestrians per hour per leg. For the sake of simplicity, the following analyses focus on pedestrians crossing only one leg of the intersection. Vehicle turning ratios and pedestrian demand level are chosen in such a way that results can be compared with previous and related studies, for example, Niels et al. (*6*, *7*) and Levin and Rey (*23*).

AIM Control Scenarios

In the evaluated scenarios, the maximum pedestrian waiting time Θ_{ped} is 42 s and all pedestrians have the same weighting factor γ_{ped} of one if not stated otherwise. Vehicle delay is not limited. The duration of the pedestrian green phase is 5.4 s. A minimum green phase duration of 5 s is prescribed by the German guideline RiLSA and is applied in several German cities, as reported by Alrutz et al. (*35*). Similar to previous papers (*6*, *7*), the green phase is only intended for pedestrians to start crossing and a longer clearance time makes sure that they can finish crossing the street safely. The assignment distance $dist^A$ is chosen to be 50 m, which allows for vehicles to slow down and accelerate without compromising safety. In addition, vehicles will decelerate early enough to make pedestrians feel safe (*36*). The roll period ϕ is chosen to be 3 s. This allows for the control to run up to 3 s to find the optimal result—computation times depending on the communication range are presented in Figure 6*b*.

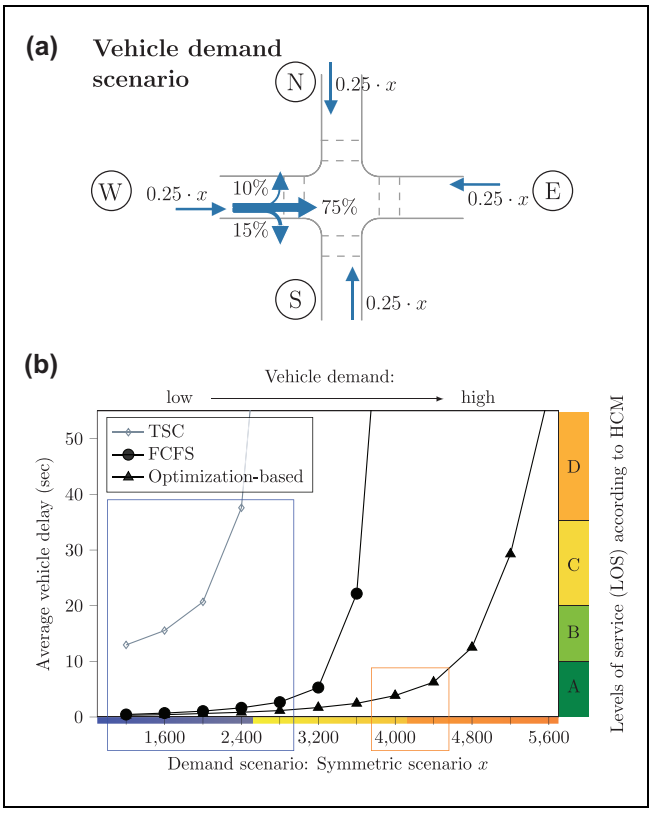

Figure 5. Demand scenarios and comparison of delays in the vehicle-only scenarios: (*a*) graphical representation of vehicle demand scenario *x* and (*b*) comparison of vehicle delays for different demand scenarios.
Note: TSC = traffic signal control; FCFS = first come, first served; HCM = Highway Capacity Manual.

Benchmark TSC Scenarios

For the vehicle-only scenarios, a fully actuated two-phase TSC is implemented for comparison. It features minimum and maximum vehicle green intervals of 22 and 52 s in each phase, which together with yellow phase and all-red times implies cycle times of 60–120 s. This corresponds to the maximum allowed cycle time in Germany (*34*).

Results and Discussion

In the following, average vehicle and pedestrian delays will be evaluated. This section first looks at vehicle-only scenarios and then focuses on the impact that different control parameters with respect to the integration of pedestrians will have.

Vehicle-Only Scenarios

First of all, the presented optimization-based scheme is compared to a FCFS control and the described fully actuated TSC for a set of vehicle-only demand scenarios. Figure 5*b* shows that AIM significantly outperforms the TSC with respect to both delays and capacity. The relatively poor performance of the TSC partly results from the small intersection layout where left-turning vehicles stopped within the intersection block the way for vehicles behind them—many reviewed papers instead consider larger intersections where the difference is less striking (*5*, *7*). The capacity can further be increased significantly using the optimization-based control. The larger capacity resulting from the optimization-based control can be used in the multimodal scenarios where a portion of space–time will be blocked for vehicles and dedicated to pedestrian movement.

Figure 6*a* shows a delay comparison for different communication ranges $dist^C$. The communication range is displayed on the *x*-axis and the average vehicle delay is shown on the *y*-axis. The two graphs correspond to the two considered demand scenarios with 4000 and 4400 vehicles per hour, respectively. In both demand scenarios, average vehicle delays decrease with increasing communication distance. On the other hand, the larger communication distance can lead to costlier optimization processes. Figure 6*b* shows that the linear increase in the number of vehicles considered in the MILP (shown by the bar plot) results in an exponential increase in computation times (shown by the line plot). As a trade-off between computation times and delay reduction, a communication distance of 150 m will be applied in the multimodal scenarios. The computation times are below the chosen roll period ϕ of 3 s and, with this setup, each vehicle is considered in at least four rounds of optimization.

In the following evaluations, scenarios with up to 2800 vehicles per hour will be considered. While this looks like a rather low demand considering the impressive results of the optimization-based AIM, it needs to be noted that it already exceeds the capacity of both the implemented TSC and the FCFS-based AIM with pedestrians introduced by Niels et al. (*6*).

Scenarios with Vehicles and Pedestrians

In the presented setup, there are three different dials that can be adjusted to balance pedestrian waiting times and vehicle delays:

1. the bounded maximum pedestrian waiting times Θ_{ped};
2. the pedestrian weighting factor γ_{ped};
3. the duration of a green phase t_{ped}^{green}.

All of these parameters ultimately influence what portion of time is dedicated to pedestrian movement. In the following, their impacts are analyzed by implementing test scenarios that are based on the analysis of the slot-based

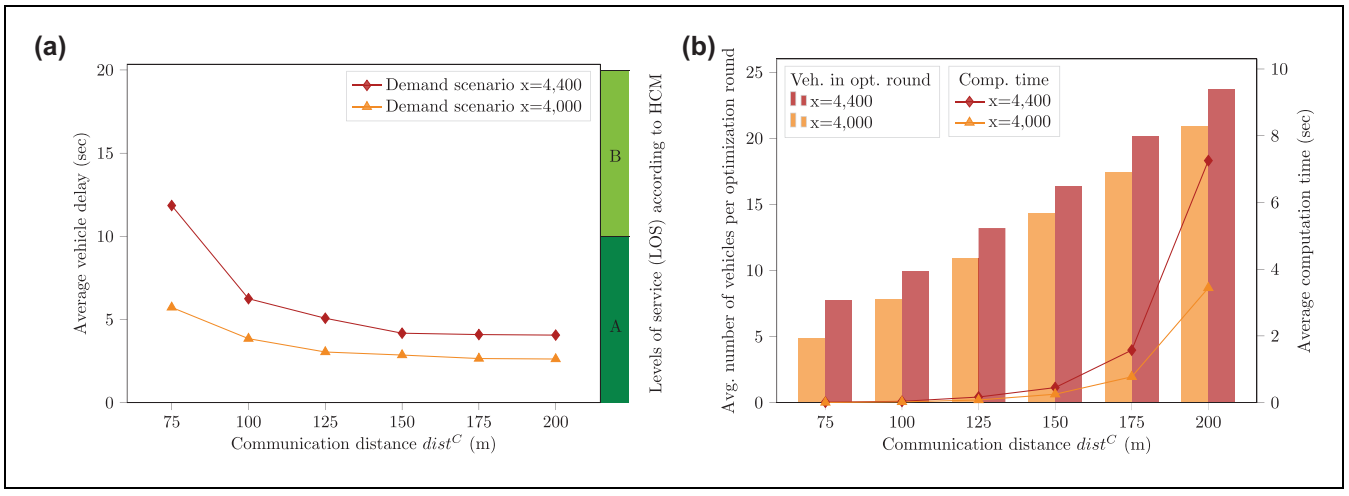

Figure 6. Impact of the communication distance on delays and computation times: (*a*) impact of the communication distance on the vehicle delay and (*b*) number of vehicles considered in each round of optimization and average computation times.
Note: The optimization was run on a Lenovo G4-i3it with Intel(R) Core(TM) i7-8665U CPU with four kernels, 2.11 GHz, and 32 GB RAM. HCM = Highway Capacity Manual.

control strategies presented in Niels et al. (*6*). The TSC results shown in Figure 5 (for vehicle delay) and analytically calculated TSC pedestrian delays based on the average cycle times and vehicle green times in the given demand scenario are shown for comparison. It needs to be noted that the presented results "oversell" the TSC, because (i) pedestrian movement is not simulated in the TSC scenario, thus neglecting delays caused by the interactions between vehicles and parallel pedestrian movement, and (ii) pedestrian green phases are usually shorter than vehicle green phases.

Impact of Maximum Pedestrian Waiting Times. Imposing the upper bound Θ_{ped} ensures that when a new pedestrian green phase is requested, this phase is started after at most Θ_{ped} s. Such an upper bound does not only have an effect on pedestrian comfort but is also safety-relevant as long waiting times can reduce pedestrian compliance with the signal (*37*). The impact of adjusting Θ_{ped} is shown in Figure 7. Figure 7*a* shows average vehicle delays for an increasing vehicle demand, while Figure 7*b* presents average pedestrian waiting times for the same scenarios, with Θ_{ped} being altered from the base scenario with 42 s to 36 and 60 s. First of all, it can be seen that the optimization-based AIM including pedestrians still significantly outperforms TSC in all demand scenarios considering vehicle delays, while pedestrian waiting times are at the same level. Furthermore, Figure 7 shows that upper bounds on pedestrian waiting times have an increasing effect with increasing vehicle demand: if vehicle demand is large, then pedestrian green phases are more often *only* scheduled after the maximum pedestrian waiting time. On the other hand, if vehicle demand is low, these upper bounds are more often redundant, because it is optimal from the control perspective to start the green phase earlier anyways. These effects can also be seen from the histograms in Figure 7, *c*–*e*, where the percentages of pedestrians with a specific waiting time (in steps of 10 s) for two different vehicle demand scenarios ($x = 1200$ and $x = 2800$) are shown for the three different values of Θ_{ped}.

Impact of Pedestrian Weighting Factor. To balance pedestrian waiting times for all considered vehicle demand scenarios, altered pedestrian weighting factors γ_{ped} are tested. Figure 8 shows results for the basic scenario with γ_{ped} equal to 1 and a scenario with γ_{ped} equal to 5. Again, average vehicle delay is shown in Figure 8*a* and average pedestrian waiting time is shown in Figure 8*b*. The larger pedestrian weighting factor reduces pedestrian waiting times in all scenarios. Even though vehicle delays increase at the same time, with γ_{ped} equal to 5, both vehicle and pedestrian delays are below the TSC baseline for all demand scenarios. Since the larger weighting factor leads to a prioritized scheduling of pedestrian green phases, they are more frequent. However, the effect cannot necessarily be generalized: If the more frequent scheduling of pedestrian signal phases at some point leads to queues in the incoming vehicle lanes, the larger number of vehicles could lead to the opposite effect and decrease the pedestrian LOS. In addition, the effect of changing pedestrian demand needs to be analyzed. If there are several pedestrians waiting at a pedestrian crosswalk, their weighting factors are added up, which also changes the overall situation.

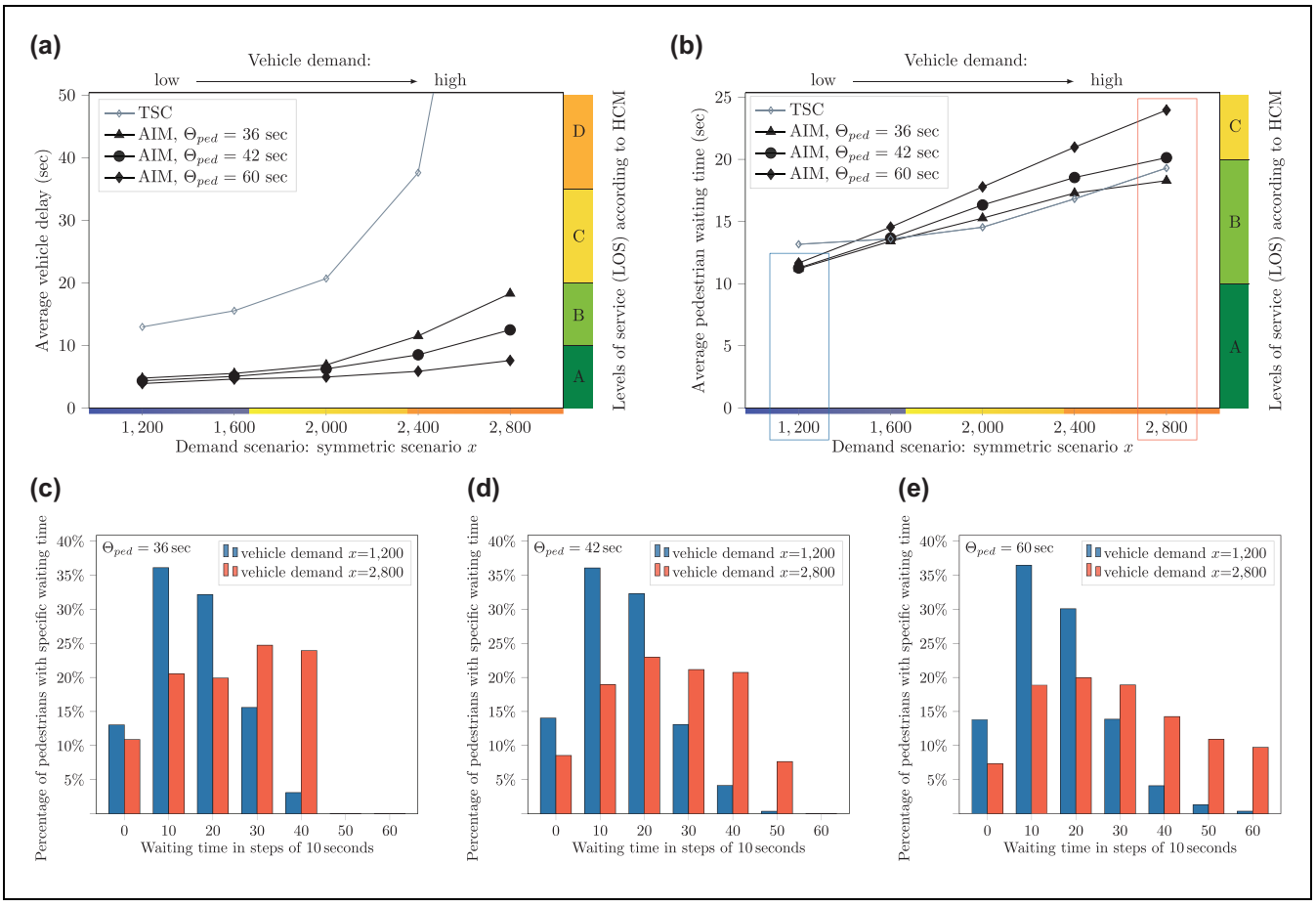

Figure 7. Average vehicle delays and pedestrian waiting times depending on vehicle demand and maximum pedestrian waiting time Υ_{ped}: (*a*) average vehicle delays depending on vehicle demand and Θ_{ped}, (*b*) average pedestrian waiting times depending on vehicle demand and Θ_{ped}, (*c*) histogram of pedestrian waiting times for $\Theta_{ped} = 36$s, (*d*) histogram of pedestrian waiting times for $\Theta_{ped} = 42$s, and (*e*) histogram of pedestrian waiting times for $\Theta_{ped} = 60$s.

Note: TSC = traffic signal control; AIM = autonomous intersection management; HCM = Highway Capacity Manual.

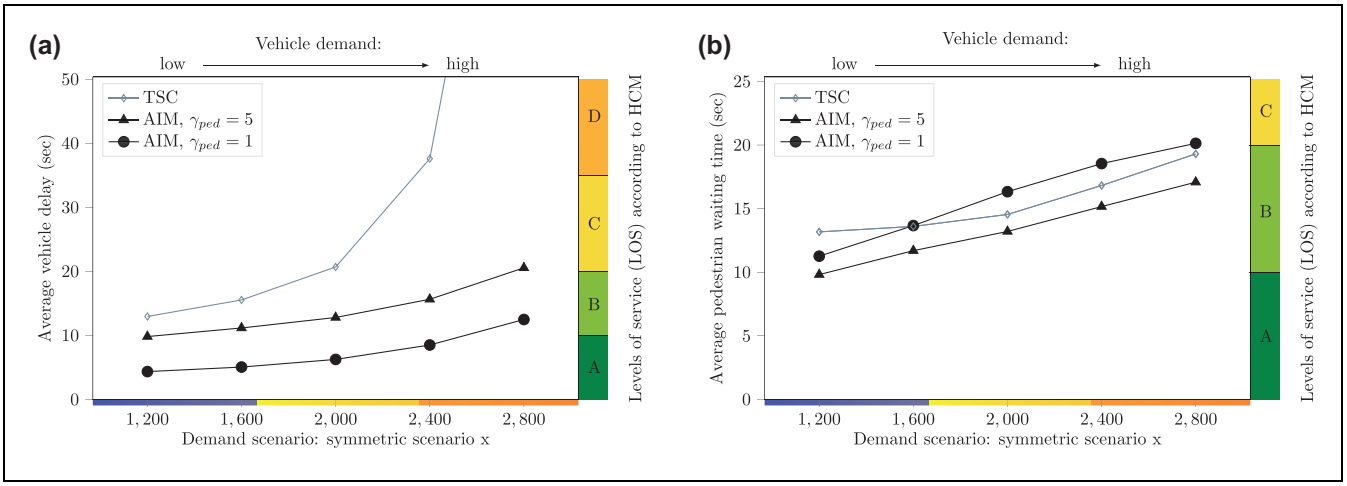

Figure 8. Average vehicle delays and pedestrian waiting times depending on vehicle demand and pedestrian weighting factor γ_{ped}: (*a*) average vehicle delays depending on vehicle demand and γ_{ped} and (*b*) average pedestrian waiting times depending on vehicle demand and γ_{ped}.

Note: TSC = traffic signal control; AIM = autonomous intersection management; HCM = Highway Capacity Manual.

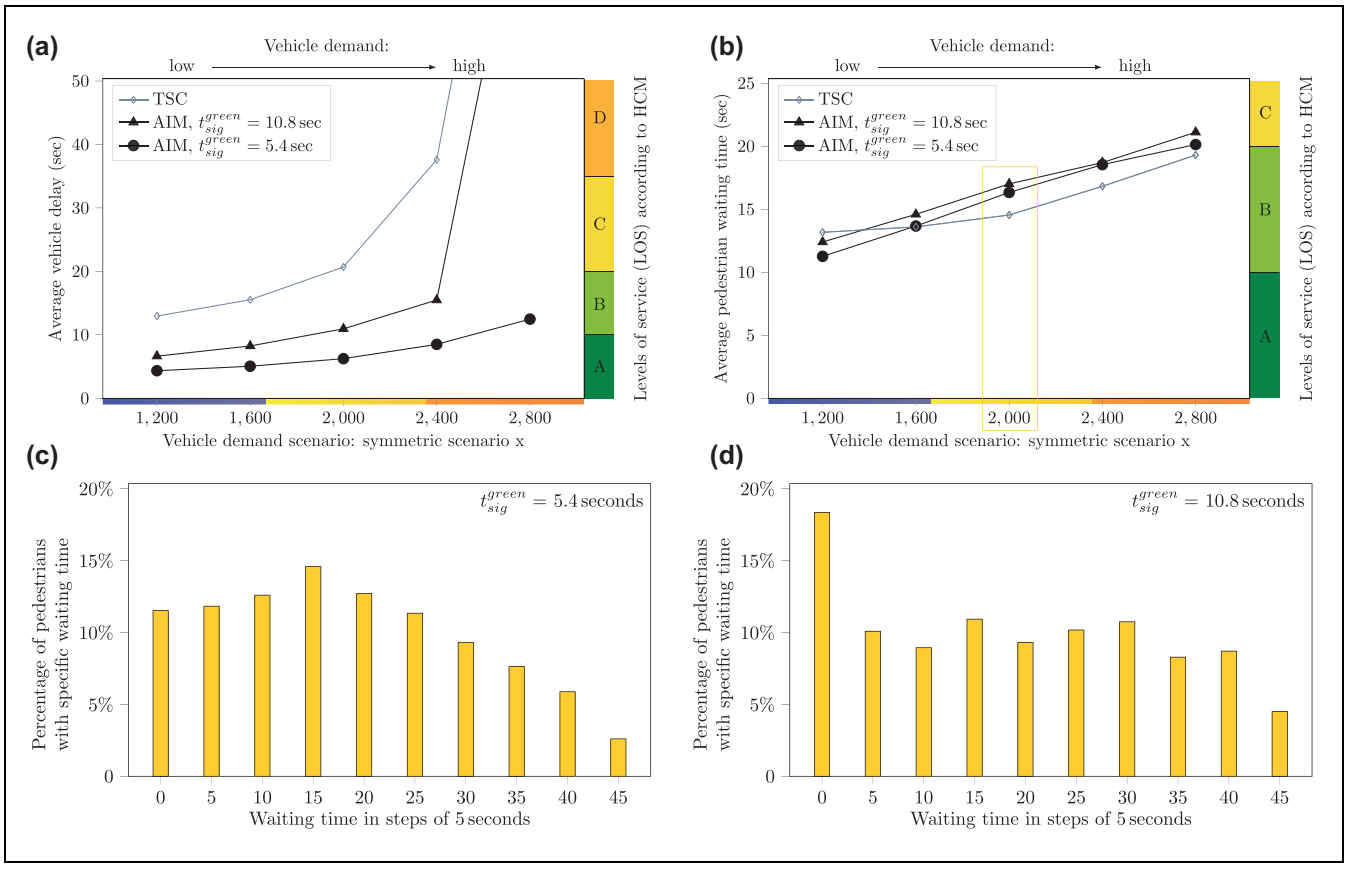

Figure 9. Average vehicle delays and pedestrian waiting times depending on vehicle demand and pedestrian green phase duration t_{sig}^{green}: (*a*) average vehicle delays depending on vehicle demand and t_{sig}^{green}, (*b*) average pedestrian waiting times depending on vehicle demand and t_{sig}^{green}, (*c*) histogram of pedestrian waiting times in steps of 5 s for $t_{sig}^{green} = 5.4$ s and symmetric vehicle demand $x = 2000$, and (*d*) histogram of pedestrian waiting times in steps of 5 s for $t_{sig}^{green} = 10.8$ s and symmetric vehicle demand $x = 2000$.
Note: TSC = traffic signal control; AIM = autonomous intersection management; HCM = Highway Capacity Manual.

Impact of Pedestrian Green Phase Duration. In the scenarios analyzed so far, each requested pedestrian signal phase has a green phase duration of 5.4 s. If a green phase is set to be longer, then the probability of a pedestrian arriving during the green phase increases. Figure 9 shows average vehicle delays and average pedestrian waiting times for increasing vehicle demand and two different green phase durations t_{sig}^{green} of 5.4 and 10.8 s. As expected, vehicle delay increases with the larger t_{sig}^{green} (see Figure 9*a*). While delays are still below the TSC scenario, the demand of 2800 vehicles per hour with t_{sig}^{green} of 10.8 s even exceeds the vehicle capacity. It might be somewhat unexpected that average pedestrian waiting times are not reduced—they are even slightly higher in the scenario with larger green phase durations. The reason is that larger green times with otherwise unchanged parameters lead to less frequent green phases, as scheduling a longer green phase is more costly from the optimization point of view. Therefore, average pedestrian waiting times are similar, but, as shown in Figure 9, *c* and *d*, the distribution is different.

Summary

Results show that the optimization-based AIM can significantly reduce delays and increase capacity in the vehicle-only scenarios. The improvements with respect to vehicle capacity and delays are also shown in scenarios where a considerable portion of time is dedicated to pedestrian movement: in the mixed scenarios, vehicle LOS can be improved in all demand scenarios while keeping pedestrian LOS on the same level as with TSC. The AIM offers several possibilities to balance vehicle and pedestrian delays. The effects depend on the interaction between different control parameters and the considered demand scenario. While differences in pedestrian waiting times might seem minor in Figures 6–8, the impact of vehicle demand on the results is clearly visible,

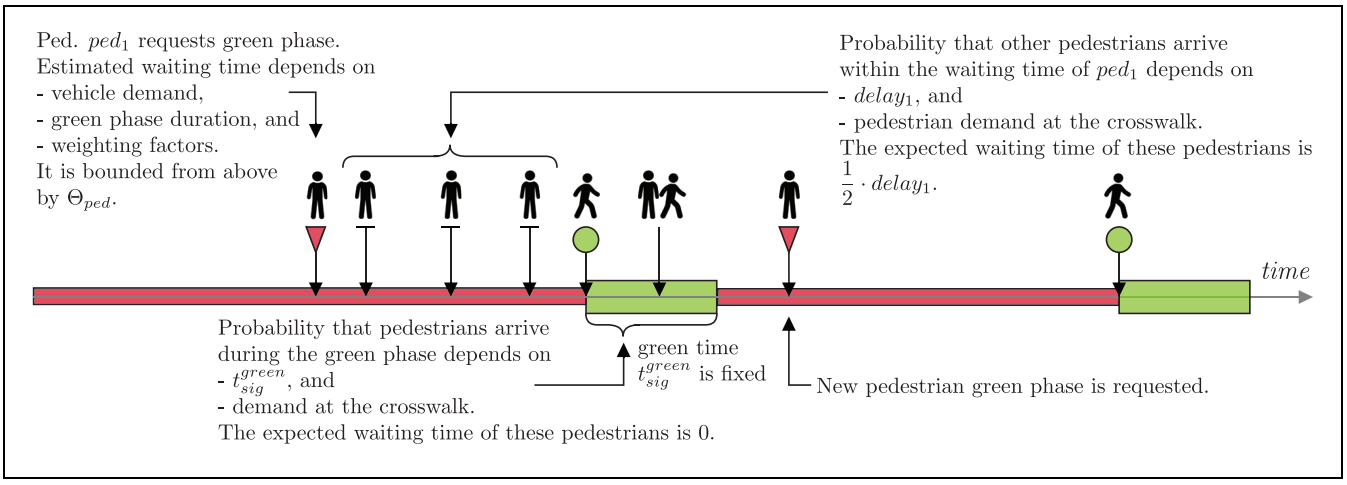

Figure 10. Schematic representation of the influence of the control parameters and demand scenario on average pedestrian waiting times.

and adjusting several parameters at the same time could lead to larger changes. The overall context is schematically displayed in Figure 10. In the figure, the first pedestrian ped_1 requests a green phase. Now, her waiting time depends on the control parameters and the situation at the intersection. If there are no approaching vehicles, the green phase can be scheduled to start immediately when the optimization is run. Otherwise, the waiting time is bounded from above by Θ_{ped}. Now, the probability that other pedestrians arrive during the time that ped_1 is waiting depends on her waiting time and on pedestrian demand. If pedestrian demand is large, more pedestrians are likely to arrive and, since their expected waiting time is shorter, the overall average pedestrian waiting time will be lower. Additional pedestrians will also increase the weighting factor γ_{sig} of the requested signal phase. Finally, the probability that pedestrians arrive during the green phase depends on the duration of the green phase and the demand at the crosswalk. Obviously, these pedestrians do not experience delay. All in all, if ped_1 is the only pedestrian, then the average waiting time will equal the waiting time of ped_1; if more pedestrians arrive before the end of the green phase, the average delay will be reduced. Finally, the frequency and duration of pedestrian green phases will also influence vehicle delays. Because of the complexity of the interdependence, once the estimated demand situation and policy objectives are clear, parameters need to be tuned for the specific situation.

Conclusion and Future Work

In this paper, an optimization-based AIM strategy for CAVs and pedestrians was explained and evaluated. Similar to previous studies of the authors, vehicles are assumed to directly sign up with the controller, while pedestrians are recognized by the infrastructure when they are at the intersection (*6*, *7*). The activation of pedestrian signal phases is fully integrated into the optimization problem. To account for limited communication distances and pedestrians not being equipped with connected devices, a rolling horizon scheme is presented and explained in detail. The simulation results confirm the significant improvements of optimization-based AIM as compared to FCFS and conventional TSC for vehicle-only scenarios. Furthermore, it is shown that these improvements even hold when considering mixed scenarios with vehicles and pedestrians while providing a pedestrian LOS that is comparable to that of TSC. In addition, the presented strategy allows for limiting pedestrian waiting times, prioritizing pedestrians via larger weighting factors in the objective function, and changing the green phase durations. A main focus was put on the demonstration and evaluation of how these control parameters can be used to balance vehicle and pedestrian delays. In the future, the control parameters can be tuned based on the considered demand situation and the policy objectives.

The proposed intersection model allows for the integration of heterogeneous vehicle types and is easily transferable to other intersection layouts. To evaluate the potentials of the control at a realistic urban intersection, we are currently working on considering diverse vehicle speeds (e.g., slower turning movements) and the integration of bicyclists into the setup. In addition, the consideration of downstream congestion and the coordination of several intersections on a road stretch or even in a network opens up new and interesting research questions.

Acknowledgments

A free Aimsun Next postgraduate license was used for conducting this research. This research is a part of the PhD thesis of T. Niels.

Author Contributions

The authors confirm contribution to the paper as follows: study conception and design: T. Niels, K. Bogenberger, M. Papageorgiou, I. Papamichail; data collection: T. Niels; analysis and interpretation of results: T. Niels, K. Bogenberger, M. Papageorgiou, I. Papamichail; draft manuscript preparation: T. Niels. All authors reviewed the results and approved the final version of the manuscript.

Declaration of Conflicting Interests

The author(s) declared no potential conflicts of interest with respect to the research, authorship, and/or publication of this article.

Funding

The author(s) received no financial support for the research, authorship, and/or publication of this article.

ORCID iDs

Tanja Niels https://orcid.org/0000-0002-8530-0285
Klaus Bogenberger https://orcid.org/0000-0003-3868-9571
Markos Papageorgiou https://orcid.org/0000-0001-5821-4982
Ioannis Papamichail https://orcid.org/0000-0002-6332-9327

References

1. TomTom International BV. TomTom Traffic Index 2019. 2020. www.tomtom.com/traffic-index. Accessed June 9, 2020.
2. European Commission. 2019 Road Safety Statistics: What is Behind the Figures? 2020. https://ec.europa.eu/commission/presscorner/detail/en/qanda_20_1004. Accessed June 19, 2022.
3. Fajardo, D., T. Au, S. Waller, P. Stone, and C. Yang. Automated Intersection Control: Performance of a Future Innovation Versus Current Traffic Signal Control. *Transportation Research Record: Journal of the Transportation Research Board*, 2011. 2259: 223–232.
4. Levin, M., S. Boyles, and R. Patel. Paradoxes of Reservation-Based Intersection Controls in Traffic Networks. *Transportation Research Part A: Policy And Practice*, Vol. 90, 2016, pp. 14–25.
5. Yu, C., W. Sun, H. Liu, and X. Yang. Managing Connected and Automated Vehicles at Isolated Intersections: From Reservation-To Optimization-Based Methods. *Transportation Research Part B: Methodological*, Vol. 122, 2019, pp. 416–435.
6. Niels, T., N. Mitrovic, K. Bogenberger, A. Stevanovic, and R. Bertini. Smart Intersection Management for Connected and Automated Vehicles and Pedestrians. *Proc., 6th International Conference on Models and Technologies for Intelligent Transportation Systems*, Cracow, Poland, IEEE, New York, 2019.
7. Niels, T., N. Mitrovic, N. Dobrota, K. Bogenberger, A. Stevanovic, and R. Bertini. Simulation-Based Evaluation of a New Integrated Intersection Control Scheme for Connected Automated Vehicles and Pedestrians. *Transportation Research Record: Journal of the Transportation Research Board*, 2020. 2674: 779–793.
8. Niels, T. *Integrated Intersection Control for Connected Automated Vehicles, Pedestrians, and Bicyclists*. PhD thesis. Technical University of Munich, Germany, 2022, pp. 1–252.
9. Dresner, K., and P. Stone. Multiagent Traffic Management: A Reservation-Based Intersection Control Mechanism. *Proc., 3rd International Joint Conference on Autonomous Agents and Multiagent Systems*, New York, NY, IEEE, Piscataway, NJ, 2004, pp. 530–537.
10. Dresner, K., and P. Stone. Human-Usable and Emergency Vehicle–Aware Control Policies for Autonomous Intersection Management. *Proc., 4th Workshop on Agents in Traffic and Transportation*, Hakodate, Japan, 2006.
11. Chen, L., and C. Englund. Cooperative Intersection Management: A Survey. *IEEE Transactions on Intelligent Transportation Systems*, Vol. 17, 2016, pp. 570–586.
12. Qian, X., F. Altché, J. Grégoire, and A. De La Fortelle. Autonomous Intersection Management Systems: Criteria, Implementation and Evaluation. *IET Intelligent Transport Systems*, Vol. 11, 2017, pp. 182–189.
13. Khayatian, M., M. Mehrabian, E. Andert, R. Dedinsky, S. Choudhary, Y. Lou, and A. Shirvastava. A Survey on Intersection Management of Connected Autonomous Vehicles. *ACM Transactions on Cyber-Physical Systems*, Vol. 4, 2020, pp. 1–27.
14. Zhong, Z., M. Nejad, and E. Lee. Autonomous and Semi-autonomous Intersection Management: A Survey. *IEEE Intelligent Transportation Systems Magazine*, Vol. 13, 2021, pp. 53–70.
15. Dresner, K., and P. Stone. A Multiagent Approach to Autonomous Intersection Management. *Journal of Artificial Intelligence Research*, Vol. 31, 2008, pp. 591–656.
16. Chen, R., J. Hu, M. Levin, and D. Rey. Stability-Based Analysis of Autonomous Intersection Management with Pedestrians. *Transportation Research Part C: Emerging Technologies*, Vol. 114, 2020, pp. 463–483.
17. Wang, M., C. Wen, and H. Chao. Roadrunner + : An Autonomous Intersection Management Cooperating with Connected Autonomous Vehicles and Pedestrians with Spillback Considered. *ACM Transactions on Cyber-Physical Systems*, Vol. 6, 2021, pp. 1–29.
18. Wu, W., Y. Liu, W. Hao, G. Giannopoulos, and Y. Byon. Autonomous Intersection Management with Pedestrians Crossing. *Transportation Research Part C: Emerging Technologies*, Vol. 135, 2022, p. 103521.
19. Li, B., Y. Zhang, Y. Zhang, N. Jia, and Y. Ge. Near-Optimal Online Motion Planning of Connected and Automated Vehicles at a Signal-Free and Lane-Free Intersection. *Proc., IEEE Intelligent Vehicles Symposium*, Changshu, China, IEEE, New York, 2018, pp. 1432–1437.

20. Dresner, K. AIM: Autonomous Intersection Management. *Proc., 7th International Joint Conference on Autonomous Agents and Multiagent Systems*, Estoril, Portugal, 2008.
21. Levin, M., H. Fritz, and S. Boyles. On Optimizing Reservation-Based Intersection Controls. *IEEE Transactions on Intelligent Transportation Systems*, Vol. 18, 2016, pp. 505–515.
22. Zhu, F., and S. Ukkusuri. A Linear Programming Formulation for Autonomous Intersection Control Within a Dynamic Traffic Assignment and Connected Vehicle Environment. *Transportation Research Part C: Emerging Technologies*, Vol. 55, 2015, pp. 363–378.
23. Levin, M., and D. Rey. Conflict-Point Formulation of Intersection Control for Autonomous Vehicles. *Transportation Research Part C: Emerging Technologies*, Vol. 85, 2017, pp. 528–547.
24. Schepperle, H., K. Böhm, and S. Forster. Traffic Management Based on Negotiations Between Vehicles: A Feasibility Demonstration Using Agents. *Proc., 9th International Conference on Agent-Mediated Electronic Commerce and Trading Agent Design and Analysis*, Springer-Verlag Berlin Heidelberg, Germany, 2007, pp. 85–98.
25. Carlino, D., S. Boyles, and P. Stone. Auction-Based Autonomous Intersection Management. *Proc., 16th International IEEE Conference on Intelligent Transportation Systems*, The Hague, Netherlands, IEEE, New York, 2013.
26. Bashiri, M., and C. Fleming. A Platoon-Based Intersection Management System for Autonomous Vehicles. *Proc., IEEE Intelligent Vehicles Symposium*, Los Angeles, CA, IEEE, New York, 2017, pp. 667–672.
27. Müller, E., R. Castelan Carlson, and W. Kraus Junior. Time Optimal Scheduling of Automated Vehicle Arrivals at Urban Intersections. *Proc., IEEE 19th International Conference on Intelligent Transportation Systems*, Rio de Janeiro, Brazil, IEEE, New York, 2016, pp. 1174–1179.
28. Fayazi, S., and A. Vahidi. Mixed-Integer Linear Programming for Optimal Scheduling of Autonomous Vehicle Intersection Crossing. *IEEE Transactions On Intelligent Vehicles*, Vol. 3, 2018, pp. 287–299.
29. Transportation Research Board (TRB). *Highway Capacity Manual*. Transportation Research Board, National Research Council, Washington, D.C., 2000.
30. FGSV - Forschungsgesellschaft für Straßen- und Verkehrswesen. *Handbuch für die Bemessung von Straßenverkehrsanlagen (HBS)*. FGSV-Verlag, Cologne, Germany, 2015.
31. Williams, H. *Model Building in Mathematical Programming*. John Wiley & Sons, Hoboken, NJ, 2013.
32. Friedrich, B.The Effect of Autonomous Vehicles on Traffic. In *Autonomous Driving* (M. Maurer, J. Gerdes, B. Lenz, and H. Winner eds.), Springer, Berlin, Heidelberg, 2016, pp. 317–334.
33. Hoogendoorn, S., and W. Daamen. Free Speed Distributions for Pedestrian Traffic. Presented at 85th Annual Meeting of the Transportation Research Board, Washington, D.C., 2006.
34. FGSV - Forschungsgesellschaft für Straßen- und Verkehrswesen. *Richtlinien für Lichtsignalanlagen (RiLSA). Lichtzeichenanlagen für den Straßenverkehr*. FGSV-Verlag, Cologne, Germany, 2015.
35. Alrutz, D., C. Bachmann, J. Rudert, W. Angenendt, A. Blase, F. Fohlmeister, and P Häckelmann. Verbesserung der Bedingungen für Fußgänger an Lichtsignalanlagen. *Berichte der Bundesanstalt für Straßenwesen*, Bergisch Gladbach, Germany, 2012.
36. Ackermann, C., M. Beggiato, L. Bluhm, A. Löw, and J. Krems. Deceleration Parameters and Their Applicability as Informal Communication Signal Between Pedestrians and Automated Vehicles. *Transportation Research Part F: Traffic Psychology and Behaviour*, Vol. 62, 2019, pp. 757–768.
37. Zhang, Y., S. Mamun, J. Ivan, N. Ravishanker, and K. Haque. Safety Effects of Exclusive and Concurrent Signal Phasing for Pedestrian Crossing. *Accident Analysis & Prevention*, Vol. 83, 2015, pp. 26–36.